PHOTOLUMINESCENCE STUDIES OF ALKALI-ANTIMONIDE PHOTOCATHODES

P. Saha*, O. Chubenko, and S.S. Karkare, Arizona State University, Tempe, AZ, USA

H.A. Padmore, Lawrence Berkeley National Laboratory, Berkeley, CA, USA

Abstract

Alkali-antimonide photocathodes have a very high quantum efficiency and a low intrinsic emittance, making them excellent electron sources for Energy Recovery Linacs, X-ray Free Electron Lasers, Electron Cooling, and Ultrafast Electron Diffraction applications. Despite numerous studies of their photoemission spectra, there has been nearly no conclusive experimental investigation of their basic electronic and optical properties (e.g. band gap, electron affinity, optical constants, etc.), which determine the nature of photoemission. Therefore, the systematic study and deep understanding of fundamental characteristics of alkali-antimonide photocathodes are required in order to develop next-generation electron sources with improved crystal and electronic structures to fit specific application. Here we report on the development of an experimental setup to measure photoluminescence (PL) spectra from alkali-antimonide photocathodes, enabling estimation of a material band gap and defect state energies, and provide preliminary results for Cs_3Sb films.

INTRODUCTION

Increasing the electron beam brightness is critical to advance the performance of such linear accelerator applications like Energy Recovery Linacs, X-ray Free Electron Lasers, Electron Cooling, and Ultrafast Electron Diffraction. The intrinsic beam brightness is defined by emission mechanisms and fundamental material properties of electron sources. For example, it has been shown that the maximum possible brightness from low quantum efficiency (QE) metallic photocathodes is limited by such nonlinear photoemission processes as electron heating and multi-photon emission [1, 2].

Alkali-antimonide compounds like Cs_3Sb, K_2CsSb, and Na_2KSb have long been known for their high QE in the visible spectrum, sub-picosecond response time, and low intrinsic emittance. Furthermore, due to their low electron affinity and high QE at the photoemission threshold, it is expected that contribution of the nonlinear photoemission processes will be reduced and near-threshold operation from such compounds will enable an order of magnitude increased brightness [3]. However, a precise quantitative estimation of nonlinear effects [4] and development of methods enabling further increase in brightness require detailed experimental study of the photoemissive, structural, electronic, and optical properties of these materials.

Despite numerous measurements of QE and intrinsic emittance [3], and some investigations of the structural properties using X-ray diffraction and reflectivity [5], very little work has been performed to experimentally obtain the electronic

and optical properties of alkali-antimonide thin films. A few optical absorption and photoconductivity measurements on alkali-antimonides have been performed several decades ago [6–11]. These experiments have given us some experimental insights into the optical and electronic properties of alkali-antimonide thin films. However, there are still many undetermined parameters that are crucial for detailed modeling of photoemission from alkali-antimonide semiconductors [12]. Furthermore, the measurements made previously were primarily performed on alkali-antimonides grown in photo-multiplier tubes on insulating quartz or pyrex surfaces. The properties of such films could potentially be very different from the thin films grown in Ultra High Vacuum (UHV) chambers on metallic or semiconducting substrates typically used in electron accelerators.

The biggest challenge in measuring the optical and electronic properties of alkali-antimonides is their extreme sensitivity to vacuum conditions. Since these films oxidize rapidly in any non-UHV environment, all measurements must be performed in the UHV growth chamber or in a separate chamber connected via UHV to the growth chamber. In this paper, we report on the development of an experimental setup for PL measurements connected to an UHV alkali-antimonide growth chamber and present preliminary measurement attempts for Cs_3Sb.

EXPERIMENTAL SETUP

Growth Chamber

Figure 1 shows the UHV chamber used for the growth of alkali-antimonides along with the setup used for PL measurements. This chamber has been used in the past for a co-deposition growth of alkali-antimonide films and is connected via UHV to an AFM/KPFM instrument for studying the surface morphology of these films [13]. The chamber uses an effusion cell to evaporate Sb metal on to a substrate (typically Si) and SAES getters to evaporate alkali-metals to form alkali-antimonide thin films. The chamber has a base pressure in the low 10^{-10} Torr range.

PL Measurement Setup

A 520 nm 1 W CW diode laser is focused onto a 100 μm rms spot on the sample to induce the PL. The laser light is incident at an angle of 30° to the normal to the sample surface. During and after the growth, the sample faces a 4-1/2 inch viewport, which is used for collecting the PL spectra.

A double convex lens system is used for collecting the light emitted by the sample into the spectrometer [14]. A schematic of this system is shown in Figure 2. Collecting the

MOPLH09

03: Novel Particle Sources and Acceleration Techniques
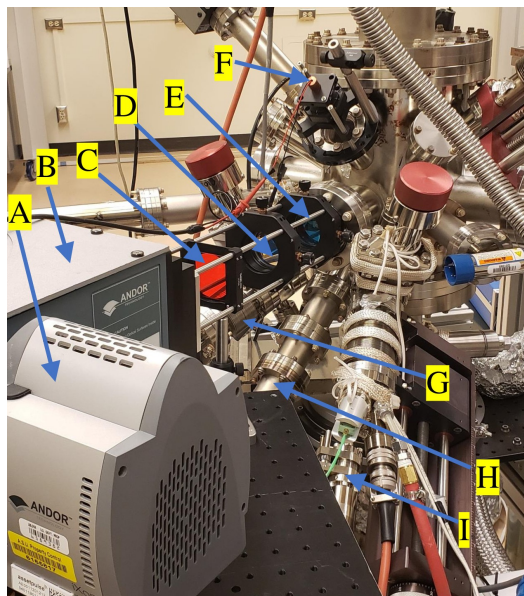
Figure 1: Experimental setup for growth of alkali-antimonide films and measurement of their PL spectra: (A) camera, (B) spectrometer, (C) low pass filter, (D) lens (f= +200mm), (E) lens (f= +250mm), (F) diode laser, (G, I) Cs sources, and (H) Sb source.

maximum amount of light emitted by the sample requires placing a convex lens with the largest possible diameter as close to the sample as possible. Without placing a lens in vacuum, the closest location for the lens placement is immediately outside the 4-1/2 inch view port making it 250 mm from the sample. The size of the viewport window is about 2 inches in diameter, making 2 inches as the most optimal lens diameter for collecting the light. The focal length of this lens is equal to the distance between the lens and the sample (250 mm), and hence it effectively collimates all the light that is collected. Then a second convex lens is used to focus the collimated light into the slit of a spectrometer. A 600 nm long pass filter is used to cut the 520 nm excitation wavelength from entering into the spectrometer slit.
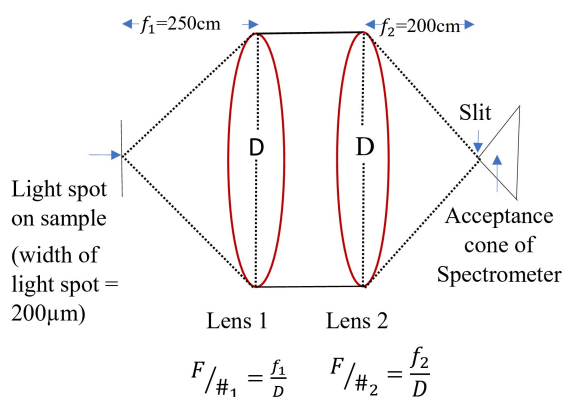
Figure 2: Diagrammatic representation for optical coupling into the spectrometer.

The spectrometer used here, the Andor Shamrock SR 303i-A, has an acceptance numerical aperture of 4. For most efficient coupling of light into the spectrometer, the numerical aperture of the second lens must match the numerical aperture of the spectrometer. Given the numerical aperture and the diameter of 2 inches, the focal length of the second lens for optimal coupling is 200 mm. This makes the spot size on the slit equal to 80 μm rms.

The spectrometer uses a grating with 300 lines/mm for diffraction and the Andor Ixon CCD camera (Model No: DV885KCS-VP) is capable of detecting single photon counts. This setup with an entrance slit width of 100 μm gives a wavelength resolution better than 1 nm. This resolution was verified using a sharp line from a green diode laser. With this entrance slit width and a spot size of 80 μm rms on the slit, around 47% of the light incident on the slit enters the spectrometer.

Assuming the sample emits light uniformly in the 2π solid angle, the first lens collects 0.5% of the emitted light. Thus, accounting for the slit width, only 0.25% of the emitted light enters the spectrometer. Less than 1 nW of 800 nm (4×10^9 photons/sec) light with FWHM spread of 1 nm was focused into the slit of the spectrometer. A strong signal could be detected with an acquisition time of 1 second. This implies that the spectrometer+camera setup is capable of detecting 4×10^9 photons/sec/nm of 800 nm light. Thus a signal of $4 \times 10^9/0.0025 = 1.6 \times 10^{12}$ photons/sec/nm emitted from the sample should be detectable by the spectrometer.

0.5 W of light at 520 nm implies 1.3×10^{18} photons/sec. Thus, for a PL signal to be detectable in one second of acquisition time, the luminescence process must have a quantum efficiency of greater than $(1.6 \times 10^{12} \times 10)/(1.3 \times 10^{18}) \approx 10^{-5}$/nm at 800 nm. The factor of 10 in the numerator has been included to account for various optical transmission and mis-alignment related losses. Allowing for the acquisition time of up to 1000 seconds, the smallest PL quantum efficiency should be greater than 10^{-8}/nm at 800 nm for detection in our setup. The camera detection efficiency at 1070 nm is nearly two orders of magnitude lower [15]. Hence, the smallest PL quantum efficiency should be greater than 10^{-6}/nm at 1070 nm for detection in our setup.

Figure 3 shows the PL spectrum from p-type GaAs ($p = 9 \times 10^{18}$ cm^{-3}) at room temperature. The measured band gap of about 1.37 eV is in a good agreement with the well-established direct band-gap of heavily p-doped GaAs (see, for example, Ref. [16]).

RESULTS

Cs-Sb was grown on a p-doped Si(100) substrates using the co-deposition technique [13]. The substrates were rinsed with isopropyl alcohol and then heated to 500° C in UHV for 4 hours. Sb and Cs were co-evaporated until a maximum QE of about 0.3% at 532 nm was achieved. We believe the low QE in this case was due to the depletion of the Cs sources.

Figure 4 shows the PL spectra obtained from the Si substrate with and without the Cs-Sb film. The spectra have
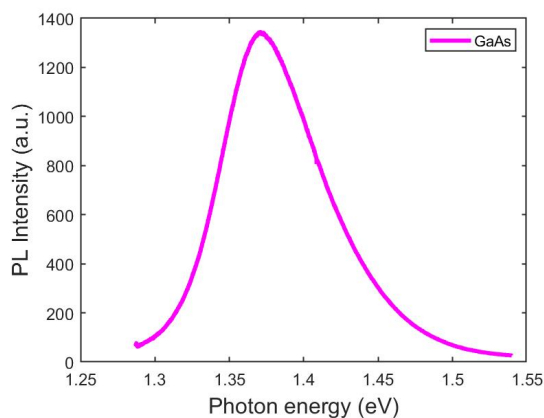
Figure 3: PL spectrum of GaAs at room temperature.
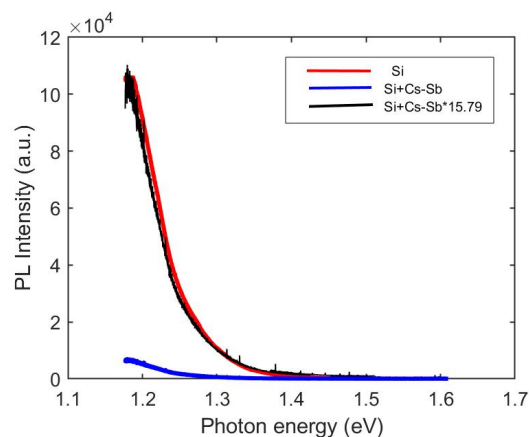
Figure 4: PL spectra of the Si substrate before and after Cs-Sb growth.

been normalized by the detection efficiency of the camera at various wavelengths [15]. Owing to the indirect band gap, Si has a very poor PL efficiency and emits light at about 1100 nm. Despite the low efficiency, we can observe the tail of the PL from the Si substrate as seen in Figure 4 (red curve). The peak of the Si spectrum cannot be observed due to the vanishingly-low sensitivity of the camera in the 1100 nm wavelength region. All spectra were taken for an acquisition time of 1000 seconds.

The spectrum after the growth of the Cs-Sb film looks identical in shape, but has a factor of ∼ 15 lower intensity (blue and black curves in Figure 4) compared to the spectra from the Si substrate prior to growth. This indicates that the Cs-Sb layer absorbs a significant portion of the incident green excitation light and/or the infrared PL from Si, however does not exhibit significant PL at wavelengths lower than 1070 nm.

Previous measurements via photoconductivity and absorption experiments have reported the band gap of Cs_3Sb to be in the range of $1.6 - 1.4$ eV [6]. Hence, Cs_3Sb can be expected to exhibit PL in the corresponding wavelengths range of $750 - 900$ nm. Despite the large absorption of light within the Cs-Sb layer, no PL signal was detected.

The lack of the expected PL signal can be a result of several factors. Firstly, the thin film grown for our experiment has a relatively low QE at green wavelengths compared to $3 - 5\%$ QE generally observed for Cs_3Sb. This could indicate the formation of phases other than Cs_3Sb that do not exhibit the expected band gap or are metallic in nature resulting in no PL. Second possibility is that the PL process in Cs_3Sb is very inefficient indicating an indirect band gap as in the case of crystalline Si. Thirdly, it is possible that Cs_3Sb has several defect states in the band gap, which mediate the electron-hole recombination processes and result either in non-radiative recombination or emission of photons with wavelength longer than 1070 nm. Lastly, it is also possible that the band structure of Cs_3Sb has low density valence bands that extend close to the conduction band, making the actual band gap less than 1.15 eV (photon energy corresponding to 1070 nm).

CONCLUSION AND FUTURE WORK

We have developed an experimental setup to measure the PL from alkali-antimonide thin films and presented preliminary results for a low-QE Cs-Sb thin film grown on a Si substrate. Despite the expected band gap of about $1.4 - 1.6$ eV for Cs_3Sb, our measurements do not show any emission in this region. This could be attributed to the various competing Cs-Sb phases that may be formed in the film, or due to the low efficiency of the PL process due to a large density of defect states.

Further experimental work is underway to grow high-QE alkali-antimonide photocathodes and study their PL properties. In particular, Cs SAES getters will be replaced with advanced effusion cells or pure metal Cs sources enabling more effective control of Cs flux during growth. Also, different alkali-metal sources will be used to grow other alkali- and multi-alkali-antimonide films. The experimental setup will be modified further (i) to perform RHEED measurements during growth permitting to distinguish between the polycrystalline and crystalline nature of the films, and (ii) to measure optical characteristics of alkali-antimonides through ellipsometry. Measured characteristics will be used for theoretical investigation of the effects limiting the performance of alkali-antimonide photocathodes. It is expected that such detailed experimental and theoretical study will shed light on the exact mechanisms affecting the emittance of alkali-antimonides and allow to develop state-of-the-art electron sources with maximized brightness.

ACKNOWLEDGEMENTS

REFERENCES

[1] J. K. Bae *et al.*, "Brightness of femtosecond nonequilibrium photoemission in metallic photocathodes at wavelengths near

the photoemission threshold," *J. Appl. Phys.* vol. 124, p. 244903, 2018.
`doi:10.1063/1.5053082`

[2] J. Maxson *et al.*, "Ultrafast laser pulse heating of metallic photocathodes and its contribution to intrinsic emittance," *Nucl. Instrum. Methods Phys. Res., Sect. A*, vol. 865, p. 99, 2017.
`doi:org/10.1016/j.nima.2016.08.032`

[3] P. Musumeci *et al.*, "Advances in bright electron sources," *Nucl. Instrum. Methods Phys. Res., Sect. A*, vol. 907, p. 209, 2018.
`doi:org/10.1016/j.nima.2018.03.019`

[4] O. Chubenko *et al.*, "Monte Carlo Study of Laser-Induced Heating Effects in GaAs Photocathodes," presented at *IVNC-IVESC'19*.

[5] S. Schubert *et al.*, "Bi-alkali antimonide photocathode growth: An X-ray diffraction study," *J. Appl. Phys.*, vol. 120, p. 035303, 2016. `doi:org/10.1063/1.4959218`

[6] W. Spicer, "Photoemissive, Photoconductive, and Optical Absorption Studies of Alkali-Antimony Compounds," *Phys. Rev.*, vol. 112, p. 114, 1958.
`doi:org/10.1103/PhysRev.112.114`

[7] E. Taft and H. Phillip, "Structure in the Energy Distribution of Photoelectrons from K_3Sb and Cs_3Sb ," *Phys. Rev.* , vol. 115, p. 1583, 1959. `doi:org/10.1103/PhysRev.115.1583`

[8] R. Nathan and C. Mee, "Photoelectric and Related Properties of the Potassium—Antimony—Caesium Photocathode," *Int. J. Electron.*, vol. 23, p. 349, 1967.
`doi:org/10.1080/00207216708961542`

[9] C. Ghosh and B. P. Varma, "Preparation and study of properties of a few alkali antimonide photocathodes," *J. Appl. Phys.*, vol. 49, p. 4549, 1978.
`doi:10.1063/1.325465`

[10] V. Beguchev *et al.*,"Optical and photoemissive properties of multi-alkali photocathodes," *J. Phys. D: Appl. Phys.*, vol. 26, p. 1499, 1993. `doi:org/10.1088/0022-3727/26/9/025`

[11] T. Sakata, "On the Thermoelectric Power of Cesium Antimonide," *J. Phys. Soc. Jpn.*, vol. 9, p. 1031, 1954.
`doi:org/10.1143/JPSJ.9.1031`

[12] P. Gupta, *et al.*,"Monte Carlo simulations of electron photoemission from cesium antimonide," *J. Appl. Phys.*, vol. 121, p. 215702, 2017. `doi:org/10.1063/1.4984263`

[13] J. Feng *et al.*,"Near atomically smooth alkali antimonide photocathode thin films," *J. Appl. Phys.*, vol. 121, p. 044904, 2017. `doi:org/10.1063/1.4974363`

[14] Tutorial on getting light into the monochromator, `https://www.newport.com/t/ getting-light-into-a-monochromator`

[15] A. Spinelli *et al.*, "Unified approach for bioluminescence, Cerenkov, β, X and γ rays imaging," *Biomed. Opt. Express*, vol. 6, p. 2168, 2015.
`doi:org/10.1364/BOE.6.002168`

[16] S. Tiwari and S. L. Wright, "Material properties of p-type GaAs at large dopings," *Appl. Phys. Lett.*, vol. 56, p. 563, 1990. `doi:10.1063/1.102745`